

# Important Role for *Mycobacterium tuberculosis* UvrD1 in Pathogenesis and Persistence apart from Its Function in Nucleotide Excision Repair

Joanna Houghton,<sup>a</sup> Carolin Townsend,<sup>b</sup> Alan R. Williams,<sup>a</sup> Angela Rodgers,<sup>c</sup> Lucinda Rand,<sup>a\*</sup> K. Barry Walker,<sup>c</sup> Erik C. Böttger,<sup>b</sup> Burkhard Springer,<sup>d</sup> and Elaine O. Davis<sup>a</sup>

Division of Mycobacterial Research, MRC National Institute for Medical Research, The Ridgeway, Mill Hill, London, United Kingdom<sup>a</sup>; Institut für Medizinische Mikrobiologie, University of Zurich, Zurich, Switzerland<sup>b</sup>; Immunology and Cellular Immunity Section, Bacteriology Division, NIBSC, South Mimms, Potters Bar, Herts, United Kingdom<sup>c</sup>; and Institute of Medical Microbiology and Hygiene, Austrian Agency for Health and Food Safety, Graz, Austria<sup>d</sup>

***Mycobacterium tuberculosis* survives and replicates in macrophages, where it is exposed to reactive oxygen and nitrogen species that damage DNA. In this study, we investigated the roles of UvrA and UvrD1, thought to be parts of the nucleotide excision repair pathway of *M. tuberculosis*. Strains in which *uvrD1* was inactivated either alone or in conjunction with *uvrA* were constructed. Inactivation of *uvrD1* resulted in a small colony phenotype, although growth in liquid culture was not significantly affected. The sensitivity of the mutant strains to UV irradiation and to mitomycin C highlighted the importance of the targeted genes for nucleotide excision repair. The mutant strains all exhibited heightened susceptibility to representatives of reactive oxygen intermediates (ROI) and reactive nitrogen intermediates (RNI). The *uvrD1* and the *uvrA uvrD1* mutants showed decreased intracellular multiplication following infection of macrophages. Most importantly, the *uvrA uvrD1* mutant was markedly attenuated following infection of mice by either the aerosol or the intravenous route.**

Tuberculosis remains a major world health problem, causing 1.75 million deaths annually (54). Furthermore, it has been estimated that one-third of the world's population is latently infected with *Mycobacterium tuberculosis* (16). Approximately 10% of those latently infected will develop active disease, but this risk is significantly increased by factors weakening the immune response, such as HIV infection (52). If latent infection in individuals at high risk of reactivation could be treated, transmission and levels of disease could be reduced dramatically. For the development of drugs active against latent bacteria, it is necessary to identify targets with functions required by the bacteria under these conditions (2).

One such function may be the ability to repair damaged DNA. In mice the continued synthesis of NO maintains the persistent state (24), in which bacterial numbers remain constant; administration of an inducible nitric oxide synthase (iNOS) inhibitor during infection results in a rapid increase in bacterial numbers (20). Thus, the bacteria must be constantly exposed to NO, which readily crosses cell membranes. Although the role of NO in human disease is less clear, it has been reported that iNOS is present and active in human tuberculosis lesions (7, 37). NO and related reactive nitrogen intermediates (RNI) damage a range of macromolecules within the cell, but it is damage to DNA that is most likely to be lethal (5, 35). These observations suggest that DNA damage must be repaired to allow the bacteria to replicate when presented with favorable conditions.

Like other bacteria, *M. tuberculosis* possesses a number of mechanisms to repair DNA: recombination, nonhomologous end joining, base excision repair, and nucleotide excision repair (NER) (14). Studies in other organisms have indicated that nucleotide excision repair is active on the kind of DNA damage produced by RNI (34, 45) and reactive oxygen intermediates (ROI) (10, 29). Furthermore, it has been shown that NER is important for resistance to NO *in vitro* in *Mycobacterium smegmatis* (22, 27) and *M. tuberculosis* (11, 12), providing the first evidence that NER performs a role in mycobacterial pathogenesis.

The process of NER begins with recognition of the damaged nucleotide by UvrA and UvrB, following which UvrA is released and UvrC is recruited by UvrB. Dual incisions of the DNA backbone either side of the damage are introduced by UvrC. Finally, release of the resulting single-stranded oligonucleotide is facilitated by the helicase UvrD, permitting resynthesis to occur (51). As well as orthologues of the three excinuclease components UvrA, UvrB, and UvrC, *M. tuberculosis* possesses two homologues of the helicase UvrD: UvrD1 and UvrD2 (8). UvrD1 is most similar to *Escherichia coli* UvrD at the amino acid sequence level (BLAST score of  $1 \times e^{-124}$  for UvrD1 compared with  $6 \times e^{-53}$  for UvrD2). UvrD2 also differs from most UvrD proteins in possessing a HRDC domain more commonly associated with RecQ family helicases (47). Furthermore, purified *M. tuberculosis* UvrD1 protein has been shown to be highly active on a substrate resembling an NER intermediate *in vitro* (9). Therefore, we hypothesized that UvrD1 is most likely functional in NER.

We targeted *uvrD1* for deletion in *M. tuberculosis* and assessed its phenotype along with that of a *uvrA* mutant described elsewhere (40). While UvrA functions solely within the NER pathway, in *E. coli* UvrD also plays a role in the mismatch repair pathway (23), which is absent in *M. tuberculosis* (49), and in recombination repair at blocked replication forks (19, 30). Our study reveals that although elimination of *uvrA* has only modest effects on pathogenicity, elimination of *uvrD1* significantly affects the chronic stage of infection, and the combined loss of both functions severely

Received 6 December 2011 Accepted 22 March 2012

Published ahead of print 30 March 2012

Address correspondence to Joanna Houghton, jdillur@nimr.mrc.ac.uk.

\* Present address: Department of Infectious Diseases and Immunity, Imperial College London, Hammersmith Campus, London, United Kingdom.

Copyright © 2012, American Society for Microbiology. All Rights Reserved.

doi:10.1128/JB.06654-11

TABLE 1 Strains and plasmids used in this study

Strain or plasmid	Relevant characteristic	Source or reference
<i>M. tuberculosis</i> strain 1424	<i>M. tuberculosis</i> wild-type H37Rv derivative, streptomycin resistant	13
$\Delta uvrA$	<i>uvrA</i> deletion mutant	40
$\Delta uvrD1$	<i>uvrD1</i> deletion mutant	This study
$\Delta uvrA uvrD$	<i>uvrA uvrD1</i> double deletion mutant	This study
pUvrD1::gm-rpsL	Targeting plasmid for removal of base pairs 299-1633 of <i>uvrD1</i> ORF	This study
Z205	<i>uvrD1</i> complementing vector, <i>uvrD1</i> in pMV361 used for <i>in vitro</i> experiments	This study
pAW33	<i>uvrD1</i> complementing vector, <i>uvrD1</i> in pKP201 used for <i>in vivo</i> experiments	This study
<i>uvrD1</i> comp	$\Delta uvrD1$ plus either Z205 or pAW33	This study

impacts the ability of *M. tuberculosis* to replicate and persist in a mouse model of infection.

## MATERIALS AND METHODS

**Bacterial strains, media, and culture conditions.** Standard procedures were adopted for cloning using *Escherichia coli* (42). The *M. tuberculosis* wild-type strain was 1424, a *rpsL* (StrR) derivative of *M. tuberculosis* H37Rv (13). *M. tuberculosis* cultures were grown in albumin, dextrose, catalase (ADC)-enriched Middlebrook 7H9 medium or modified Dubos (Difco) supplemented with albumin and 0.2% glycerol at 37°C in a rolling incubator at 2 rpm. Generation times were calculated from optical density measurements at 600 nm (OD<sub>600</sub>) of cultures in the logarithmic growth phase. When appropriate, antibiotics were added at the following concentrations: hygromycin, 50 µg/ml; kanamycin, 25 µg/ml; streptomycin, 100 µg/ml; and gentamicin, 15 µg/ml. All procedures with *M. tuberculosis* were carried out under containment level 3 conditions. The strains and plasmids used in this study are listed in Table 1.

**Isolation and complementation of mutant strains of *M. tuberculosis*.** *M. tuberculosis* mutants were generated by allelic replacement (43). For disruption of *uvrD1* (Rv0949), a 5.1-kb *Apal*/*EcoRV* fragment containing the *uvrD1* gene was isolated from bacterial artificial clone *Rv103* (4) and cloned into plasmid *ptrpA-1-rpsL* (44) previously digested with *Apal*/*EcoRV* to give *puvrD1-rpsL*. A 1.4-kb fragment (*Sall*-*AatII*) was deleted and substituted by a 3-kb gentamicin resistance cassette originally derived from plasmid pML10 (28), resulting in plasmid *puvrD1::gm-rpsL*. The deletion allele lacks base pairs 299 to 1683 of the 2,316-base pair *uvrD1* open reading frame (ORF).

To isolate mutant strains, the *uvrD1* targeting construct was transformed into *M. tuberculosis* strain 1424 or into the *uvrA* mutant selecting for chromosomal integration of the targeting plasmid using gentamicin. Following the identification of a single crossover by Southern blot analysis, counter selection on streptomycin in the presence of gentamicin was used to isolate a double crossover. Southern analysis was performed to identify *uvrD1* mutant strains using a 2,411-bp 5' probe (*HpaI*/*SacI*) with *SacI*-digested DNA.

For *in vitro* complementation experiments, the *uvrD1* gene plus 362-bp upstream and 641-bp downstream sequences was cloned from *puvrD1-rpsL* into the *HpaI* site of the integrative vector pMV361 (50), such that *uvrD1* would be transcribed in the opposite direction to the vector *hsp60* promoter. For *in vivo* complementation experiments, *uvrD1* plus 299-bp upstream and 102-bp downstream DNA was cloned into the *EcoRV* of the integrative vector pKP201 (21) that lacks the integrase to ensure high-level stability of the plasmid in *M. tuberculosis*, yielding pAW33. This plasmid was introduced into the *uvrD1* and the *uvrA uvrD1* strains by cotransformation with pBluescriptint, a suicide plasmid bearing a copy of the integrase gene (48).

**Susceptibility to DNA damaging agents, ROI and RNI.** To assess the susceptibilities of the mutant strains to both UV irradiation and *in vitro* stress, cultures were compared with that of the wild-type parental strain as previously described (40), but the cultures also included menadione (250 µM) in addition to sodium nitrite (2 mM), mitomycin C (0.1 µg/ml), and *t*-butyl hydroperoxide (0.1 mM). The OD of all cultures was determined at the start of the experiment, and approximately equal levels of inoculum were used for all strains. Serial dilutions were prepared and plated in duplicate for CFU determination. Survival was calculated by the ratio of CFU of the treated cultures compared to the CFU of the untreated controls. Three independent biological replicates were performed.

**Bone marrow macrophage isolation and infection.** Bone marrow derived macrophages (BMDMs) were generated from 6- to 8-week-old BALB/c mice in RPMI 1640 (Gibco) containing 10% fetal calf serum, 20 µM L-glutamine, 1 mM sodium pyruvate, 10 µM HEPES, and 50 nM β-mercaptoethanol. The cells were grown and differentiated in complete RPMI 1640 supplemented with 20% L929 cell supernatant for 6 days at 37°C in 5% CO<sub>2</sub>. The differentiated cells were seeded at a density of 2 × 10<sup>5</sup> cells/well in 1 ml complete RPMI 1640 supplemented with 5% L929 cell supernatant; where cells were stimulated with gamma interferon (IFN-γ), media were supplemented with IFN-γ at a concentration of 10 ng/ml. After seeding, all cells were incubated overnight prior to infection.

*M. tuberculosis* strains were grown to an OD<sub>600</sub> of 0.5 to 0.8 and inocula prepared by washing and resuspending the cultures in phosphate-buffered saline (PBS). Strains were then spun slowly at 50 × g to remove any clumps and produce a single-cell suspension. This was used to infect BMDMs at a multiplicity of infection of 1:10. After 4 h, the cells were washed to remove all extracellular bacilli, the medium was replaced, and incubation continued. Macrophages were lysed with water-0.05% Tween 80 to release intracellular bacteria at specific time points postinfection. Released bacilli were serially diluted in PBS-Tween and plated on 7H11-oleic acid-albumin-dextrose-catalase (OADC) for enumeration of surviving bacteria.

**Infection of mice.** Experiments involving mice were conducted in strict accordance with the United Kingdom Animal (Scientific Procedures) Act 1986 under licenses 80/2236, 80/2379, and 80/1927, and all efforts were made to minimize suffering. Female, specific-pathogen-free BALB/c mice (6- to 8-weeks-old) were obtained from the breeding facility at the National Institute for Medical Research (Mill Hill, United Kingdom), and the studies were performed in containment level 3 animal facilities.

For intravenous infection, logarithmically growing cultures were diluted in saline and approximately 10<sup>6</sup> CFU injected into the tail vein. The progress of the infection was assessed by determining organ CFU at various time points using four mice per strain per time point. Organs were homogenized in a FastPrep instrument (MP Biomedicals) in 5 ml of water-0.05% Tween 80 using 1/4-in. ceramic beads at a setting of 4.0 m/s for 25 s in a chilled holder.

For aerosol infection, logarithmically growing cultures were diluted to approximately 10<sup>5</sup> CFU/ml and mice were infected using an inhalation exposure system (Glas-Col) to deliver approximately 100 bacilli per mouse. Organs were homogenized in 1.2 ml of saline using the FastPrep 120 at a setting of 6.0 for 20 s. Serial dilutions of organ homogenates from five mice per strain per time point were plated on 7H11-OADC to quantify CFU.

**RNA isolation and purification.** To isolate mycobacterial RNA from *in vitro* cultures, 50 ml of culture at an OD of 0.5 to 0.8 was pelleted at 3,000 rpm for 15 min. RNA was extracted from the resulting pellet using a FastRNA Pro Blue kit (Qbiogene). To isolate mycobacterial RNA from infected mice lungs, tissue was homogenized in TRIzol using a beadbeater with (1/4-in.) beads at a setting of 6.0 for 20 s. This was then passed through a 70-µm cell strainer before being centrifuged at 13,000 rpm for 5 min. TRIzol containing host material was then removed and the resulting pellet resuspended in 1 ml TRIzol and homogenized using 150 to 200 µm glass beads at a setting of 6.0 for 40 s.

Additional RNA purification, removal of contaminating DNA, con-

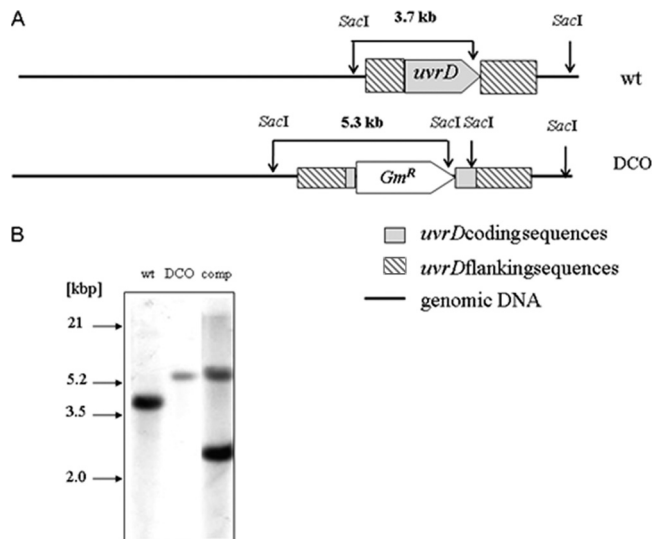


**FIG 1** Analysis of the *uvrD1* and *uvrA uvrD1* mutant genotypes by Southern blot. (A) Schematic illustration of the *uvrD1* locus and the Southern blot strategy. Shown are the genomic organization of the wild type (WT) and the mutated genomic *uvrD1* region in the double crossover mutant (DCO). Fragments detected by the probe specific for the 5' flanking region are shown in bold. (B) Southern blot hybridized with a *uvrD1*-specific probe. Genomic DNA from the *M. tuberculosis* wild type (lane 1), the *uvrD1* mutant (lane 2), and the complemented *uvrD1* mutant (lane 3) was digested with *SacI* and probed with a 2,411-bp *HpaI/SacI uvrD1* gene fragment. The presence of a single 5.3-kb fragment instead of a 3.7-kb fragment demonstrates successful deletion of *uvrD1* coding sequences. Complementation of *uvrD1* is indicated by an additional hybridization signal at 2.4 kbp. Inactivation of the *uvrA* locus in the *uvrA uvrD1* mutant was also confirmed by Southern blot analysis (data not shown).

version to cDNA and quantitative real-time PCR (qRT-PCR) were performed as described previously (18).

**Statistical analyses.** Data were log transformed prior to statistical testing so that they would more closely follow a normal distribution. Statis-

tical significance of the difference between experimental groups was then assessed by one-way analysis of variance (ANOVA) applying Tukey's multiple comparison test using Prism 4 (GraphPad), except in the case of the UV survival experiment where two-way ANOVA was performed followed by Bonferroni posttests.

## RESULTS

**Isolation of mutant strains and complementation.** The strains containing mutations in *uvrD1* alone or in conjunction with *uvrA* were constructed (43) as described in Materials and Methods. For each mutant strain, the deletion was confirmed by Southern analysis (Fig. 1). The *uvrD1* gene was expressed from its own promoter in an integrating plasmid for complementation, as detailed in Materials and Methods.

**The *M. tuberculosis uvrD1* and *uvrA uvrD1* mutants have altered colony morphology.** The *uvrD1* and *uvrA uvrD1* mutants differed from the wild type by changes in colony morphology, most noticeably in colony size (Fig. 2A). These colonies were markedly smaller than those of the wild-type or the complemented *uvrD1* strain. Despite the differences in colony size, growth in liquid culture, as assessed by optical density measurements, displayed no statistically significant difference between the strains (Fig. 2B).

**The *M. tuberculosis* NER mutants have enhanced susceptibility to DNA damaging agents.** As *M. tuberculosis* contains two UvrD homologues, of which UvrD1 is most similar to UvrD of *E. coli*, we undertook experiments to confirm that UvrD1 is involved in NER. NER is particularly important for the repair of intrastrand cross-links, such as cyclobutane pyrimidine dimers commonly formed as a result of UV irradiation, and interstrand cross-links caused by bifunctional chemical reagents, such as mitomycin C (39). Therefore, the susceptibilities of the mutant strains to UV light and mitomycin C were assessed and compared with those of the parental strain.

The *uvrA* mutant was highly sensitive to UV light at doses which had only minor effects on the wild-type strain, and inacti-

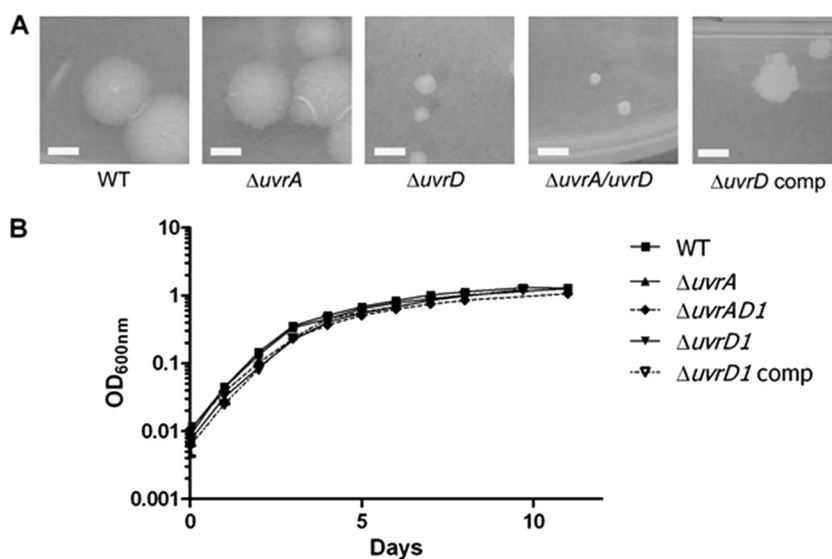


**FIG 2** *In vitro* growth characteristics of the *uvrD1* and *uvrA uvrD1* mutant strains. (A) The colony size and morphology of the *uvrD1* and *uvrA uvrD1* strains are compared with the wild type, the *uvrD1* complement, and a *uvrA* mutant, demonstrating the reduced colony size caused by inactivation of *uvrD1*. In each case the white bar in the image represents 3 mm, and the images were taken after 3 weeks of growth at 37°C. (B) Growth of the strains in liquid culture was compared with that of the wild-type parental strain by measuring optical density.

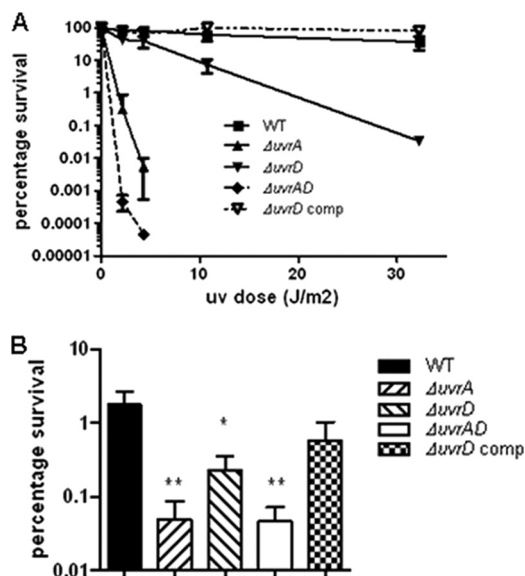


**FIG 3** Sensitivity of the *uvrD1* and *uvrA uvrD1* mutant strains to DNA damage. Survival of the *uvrD1* and *uvrA uvrD1* strains following DNA damage caused by UV irradiation (A) or mitomycin C (B) was compared with that of the wild type, the *uvrD1* complement, and a *uvrA* mutant. Survival following exposure to the indicated agent was assessed as described in Materials and Methods. In each case the surviving fraction was calculated by comparison with an untreated control. The data shown are the means of duplicate (UV) or triplicate (mitomycin C) assays from three biological replicates; the error bars represent standard deviations. One hundred percent survival in each case corresponds to approximately  $10^7$  CFU. The data in panel A for the *uvrA* and *uvrA uvrD1* strains at all UV doses were significantly different from the wild type ( $P < 0.001$ ; ANOVA). Survival of each mutant strain in panel B was significantly different from the wild type (\*,  $P < 0.05$ ; \*\*,  $P < 0.01$ ; ANOVA).

vation of *uvrD1* in addition to *uvrA* resulted in enhanced susceptibility to UV irradiation ( $P < 0.001$ ) (Fig. 3A). The *uvrD1* mutant also exhibited greater sensitivity to UV than the wild type, although to a lesser degree than the *uvrA* mutant. The difference in sensitivity from the wild type was statistically significant at the higher doses tested ( $P < 0.001$ ) (Fig. 3A). Survival of the *uvrD1* mutant was restored by complementation ( $P > 0.05$  compared with the wild type).

Similarly, the *uvrA* and *uvrA uvrD1* mutant strains were significantly ( $P < 0.001$ ) more sensitive to mitomycin C than the wild-type strain (Fig. 3B). Again, the *uvrD1* mutant exhibited an intermediate level of susceptibility to this form of DNA damage compared with the *uvrA* mutant and the wild type ( $P < 0.05$  compared with the wild type), and survival similar to the wild type was restored by complementation with *uvrD1*.

These results parallel the reported phenotypes for *uvrA* and *uvrD* mutants in *E. coli* (25, 53) and suggest that *uvrD1* is the homologue involved in NER in *M. tuberculosis*.

**The *M. tuberculosis* NER mutants exhibit elevated sensitivity to ROI and RNI.** During infection, DNA damage can be caused by ROI and/or RNI. Therefore, we investigated whether the mutant strains were more susceptible to representative agents generating such stresses.

The *uvrA* and *uvrA uvrD1* mutant strains were highly sensitive to nitrosative stress (Fig. 4A), with survival being reduced by 500-fold and 2,000-fold, respectively, relative to that of the wild type ( $P < 0.001$ ). Similar to the observations reported above for the

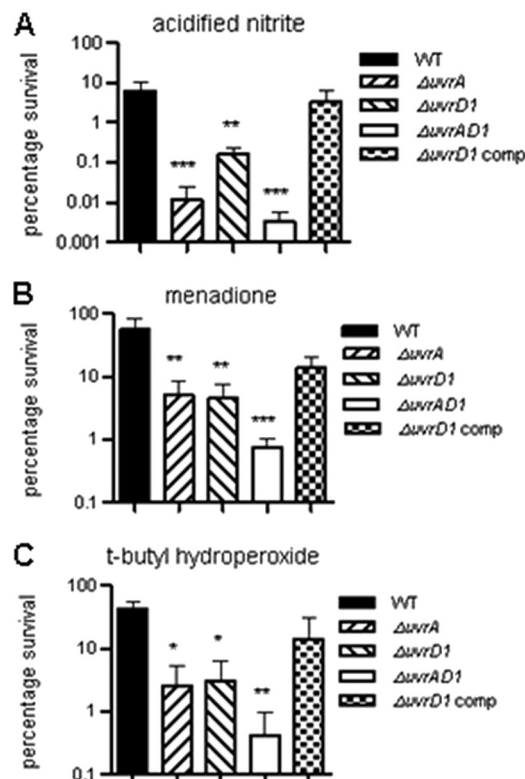


**FIG 4** Susceptibility of the *uvrD1* and *uvrA uvrD1* mutant strains to nitrosative and oxidative stresses. Survival of the *uvrD1* and *uvrA uvrD1* strains following exposure to acidified sodium nitrite (A), *t*-butyl hydroperoxide (B), or menadione (C) was compared with that of the wild type, the *uvrD1* complement, and a *uvrA* mutant. Survival following exposure to the indicated agent was assessed as described in Materials and Methods. In each case the surviving fraction was calculated by comparison with an untreated control. The data shown are the means of triplicate assays from three biological replicates; the error bars represent standard deviations. One hundred percent survival in each case corresponds to approximately  $10^7$  CFU. The data for each mutant was significantly different from that for the wild type for each stress condition (\*,  $P < 0.05$ ; \*\*,  $P < 0.01$ ; \*\*\*,  $P < 0.001$ ; ANOVA).

standard DNA damaging agents, the susceptibility of the *uvrD1* mutant to nitrosative stress was less severe than for the other mutants, although it was still 40-fold more sensitive than the wild type ( $P < 0.01$ ); this enhanced sensitivity was restored to a near-wild-type level by complementation ( $P > 0.05$  compared with the wild type).

All three of the mutant strains were also more sensitive than the wild type to both *t*-butyl hydroperoxide and menadione but to a lesser extent than was the case for nitrosative stress (Fig. 4B and C). In the case of oxidative stress, the susceptibilities of the *uvrA* and *uvrD1* mutants were similar to each other, with survival being reduced 11- to 12-fold in the case of menadione ( $P < 0.01$ ) and 14- to 16-fold with *t*-butyl hydroperoxide ( $P < 0.05$ ) relative to the wild type. In contrast, the *uvrA uvrD1* strain was 73-fold ( $P < 0.001$ ) and 98-fold ( $P < 0.01$ ) more sensitive than the wild type to menadione and *t*-butyl hydroperoxide. Again, the phenotype of the *uvrD1* mutant was restored to a near-wild-type level by complementation ( $P > 0.05$  compared with the wild type).

Thus, NER in *M. tuberculosis* is important for the repair of damage caused by RNI and to a lesser extent by ROI and so might be expected to contribute to survival during infection.

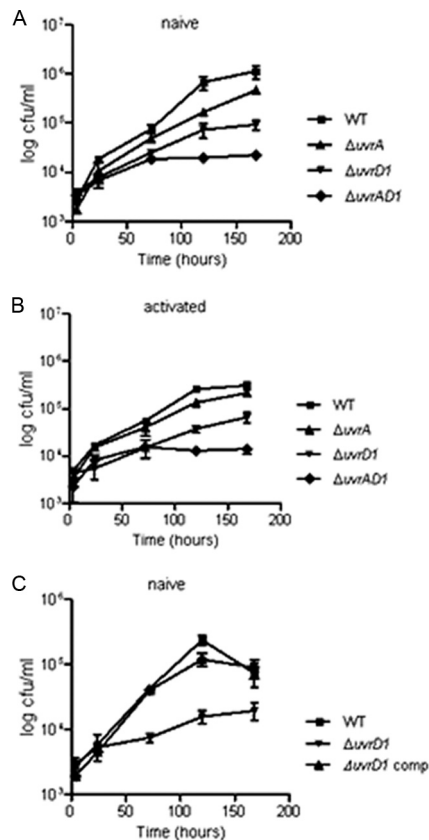


**FIG 5** Attenuation of the *uvrD1* and *uvrA uvrD1* mutant strains in a macrophage model of infection. Growth and survival of the *uvrA*, *uvrD1*, and *uvrA uvrD1* strains were compared with those of the wild type following infection of naïve macrophages (A and C) and IFN- $\gamma$ -activated mouse bone-marrow-derived macrophages (B). Macrophages were isolated and infected as detailed in Materials and Methods. Bacterial numbers were determined at specific time points up to a maximum of 7 days postinfection. Each experiment was performed at least three times with similar results; the results of a representative experiment are shown, for which the data are the means of CFU determinations performed on triplicate infections, and the error bars represent standard deviations. The data from the *uvrD1* and *uvrA uvrD1* mutants were significantly different from those for the wild type from day 3 onwards ( $P < 0.05$ ; ANOVA).

**The *uvrD1* and the *uvrA uvrD1* mutants showed decreased intracellular multiplication following infection of macrophages.** To investigate the function of NER during infection, we initially used a cell-based model. Both naïve and IFN- $\gamma$  activated macrophages were infected with each strain, and the progress of infection was monitored.

The wild-type strain reproducibly replicated to levels corresponding to an increase of at least 100-fold the initial bacterial number during the course of the experiment. Growth and survival of the *uvrA* mutant was very similar to that of the wild type, but the *uvrD1* and *uvrA uvrD1* strains were unable to reach such high bacterial loads (Fig. 5A and B). At the end of the experiment, the bacterial numbers recovered from naïve infections with the *uvrD1* and the *uvrA uvrD1* mutants were consistently lower than those for the wild type (12- to 18-fold and 16- to 50-fold lower, respectively) ( $P < 0.001$ ). When macrophages were IFN- $\gamma$  stimulated, bacterial numbers were lower for all strains with the *uvrD1* and the *uvrA uvrD1* mutants remaining less able to replicate than the wild

type. Bacterial numbers for the *uvrD1* and the *uvrA uvrD1* mutants were 3- to 6-fold ( $P < 0.05$ ) and 14- to 29-fold ( $P < 0.001$ ) lower, respectively, than for the wild type. Complementation of the *uvrD1* mutant restored the ability to survive in macrophages to wild-type levels (Fig. 5C).

**The *uvrD1* and the *uvrA uvrD1* mutants are attenuated following infection of mice.** To determine the role of NER in pathogenesis in whole animals, two mouse models of infection were used: a low-dose aerosol challenge model and an intravenous challenge model to assess complementation.

BALB/c mice were infected with each strain by the aerosol route (Fig. 6A and B). The bacterial load of the *uvrA* mutant was only slightly less than that of the wild type throughout the course of infection. However, the *uvrD1* mutant exhibited a strongly attenuated phenotype, with consistently lower CFU after day 50 in both the lungs and the spleen ( $P < 0.001$  compared with the wild type), indicating attenuation at the later stages of infection. Strikingly, the *uvrA uvrD1* mutant was highly attenuated throughout the course of infection ( $P < 0.001$  compared with the wild type), showing very limited replication in the lungs and with CFU in the spleen being close to the limit of detection at all time points analyzed.

To confirm that inactivation of *uvrD1* in the *uvrA uvrD1* double mutant was responsible for the attenuation observed, *uvrD1* was complemented and an intravenous infection of mice was performed (Fig. 6C and D). The patterns of growth for the strains were similar to those seen in the aerosol infection experiment. The *uvrD1* mutant failed to reach as high a bacterial burden as the wild type ( $P < 0.01$ ), and CFU declined at later time points in the spleens, but this phenotype was restored upon complementation ( $P > 0.05$  compared with the wild type). The *uvrA uvrD1* mutant again was severely defective in its ability to establish an infection ( $P < 0.001$  compared with the wild type). In contrast, complementation of *uvrD1* restored the ability of the bacteria to replicate in the mouse to a level similar to that observed for the *uvrA* mutant ( $P > 0.05$ ). This demonstrates that the severe attenuation of the *uvrA uvrD1* strain is due to inactivation of *uvrD1* in the absence of a functional NER system.

**Expression of *uvrD1* is increased in late infection.** To address the importance of UvrD1 in persistence, *uvrD1* expression was assessed by qRT-PCR from 3 and 22 weeks infection of mice with wild-type *M. tuberculosis*. These time points correspond to acute and chronic stages of infection, respectively (Fig. 7). It was observed that *uvrD1* was upregulated 5.6-fold in early infection compared to *in vitro* expression levels. Expression of *uvrD1* was then further upregulated in late infection, increasing to 128-fold the *in vitro* levels. These observations support the importance of UvrD1 during infection, particularly in the chronic stage.

## DISCUSSION

This study set out to address the role of NER in the pathogenicity of *M. tuberculosis* by targeting *uvrD1* for inactivation in both a wild-type strain and an isogenic *uvrA* mutant strain. UvrA is part of the damage recognition complex while UvrD is the helicase involved in the final stages of oligonucleotide displacement prior to repair synthesis (51).

Published data demonstrate that *E. coli* UvrD is required for mismatch repair (23) (which is absent in mycobacteria [49]), NER (26), replication restart, and recombination (19, 30). Up until now there has been no direct evidence for the involvement of

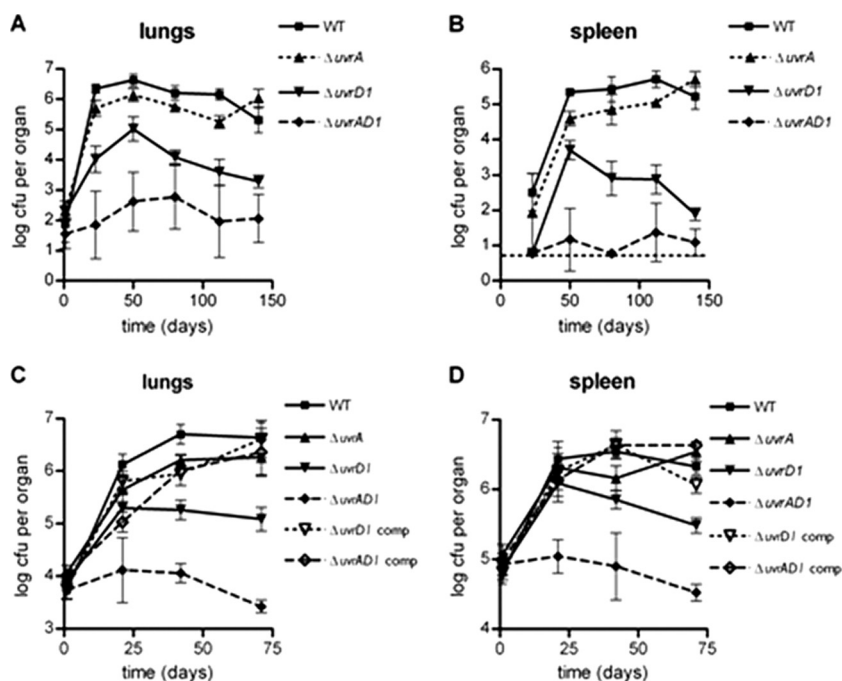


**FIG 6** Attenuation of the *uvrD1* and *uvrA uvrD1* mutant strains in mouse models of infection. Growth and survival of the *uvrD1* and *uvrA uvrD1* strains were compared with the wild type and a *uvrA* mutant following infection of BALB/c mice as detailed in Materials and Methods. (A and B) Infection by the aerosol route; CFU were enumerated from the lungs and spleens of five mice for each time point. The data for the *uvrA uvrD1* mutant were significantly different from the corresponding values for the wild type ( $P < 0.001$ ), the *uvrA* mutant ( $P < 0.001$ ), and the *uvrD1* mutant ( $P < 0.01$ ) at all time points in the lungs and at each time point after day 50 in the spleens. The data for the *uvrD1* mutant were significantly different from those for the wild type in both organs at each time point after day 50 ( $P < 0.001$ ). (C and D) Infection by the intravenous route; additional strains in which the *uvrD1* and *uvrA uvrD1* mutants were complemented with *uvrD1* were included in the analysis. Bacterial loads were determined from the lungs and spleens of four mice for each time point. The data for the *uvrA uvrD1* mutant were significantly different from the corresponding values for the wild type ( $P < 0.001$ ), the *uvrA* mutant ( $P < 0.001$ ), the *uvrD1* mutant ( $P < 0.01$ ), and both the complemented strains ( $P < 0.001$ ) at all time points in both organs. The data for the *uvrD1* mutant were significantly different from those for the wild type and its complemented strain in both organs from day 42 onwards ( $P < 0.01$ ). In each case the mutant strains showed similar phenotypes in a second independent experiment; the results shown are the means, and the error bars represent standard deviations.

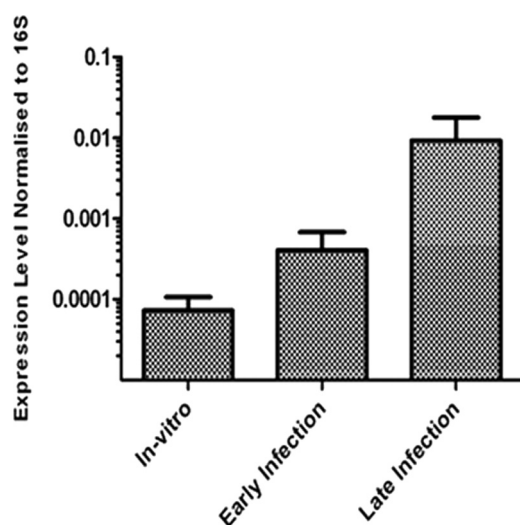


**FIG 7** Expression of *uvrD1* during mouse infection by qRT-PCR. Expression level of *uvrD1* was measured from *in vitro* exponential cultures, early mouse infection (3 weeks), and late mouse infection (22 weeks). Expression level was normalized to that of 16S. The results shown are the means of 3 biological replicates, and the error bars represent standard deviations.

UvrD1 in nucleotide excision repair in *M. tuberculosis*. However, biochemical studies of *M. tuberculosis* UvrD1 have shown it to be a helicase with 3'-5' polarity and with an unwinding preference for nicked DNA duplexes that resemble that of NER intermediates in addition to substrates resembling stalled replication forks (9), and a recent study has implicated a role for *M. smegmatis* UvrD1 in recombination (22).

UvrD1, having the closest sequence similarity to *E. coli* UvrD, was selected for inactivation. Inactivation of *uvrD1* led to a pronounced reduction in colony size. However, growth in liquid culture was not affected, with no significant difference in doubling times between strains. Our demonstration of enhanced susceptibility of the *uvrD1* mutant to UV and mitomycin C, which generate DNA damage classically repaired by NER, along with the restoration of this phenotype to that of the wild type upon complementation, confirms that UvrD1 is involved in the NER pathway. The intermediate sensitivity of the *uvrD1* strain compared with the *uvrA* mutant and the wild-type strains to both these stresses is similar to the phenotype of *uvrD* mutants in *E. coli* (25, 53).

To investigate the role of NER in the repair of DNA damage generated by more physiologically relevant agents, susceptibilities to ROI and RNI were assessed. The agents used were *t*-butyl hydroperoxide, a membrane-permeant oxidant that is more stable than hydrogen peroxide (33), and menadione, a generator of su-

peroxide stress (6, 38), for ROI and acidified sodium nitrite for RNI. While all the mutant strains exhibited increased sensitivity to these stresses, in each case the *uvrA uvrD1* double mutant was most affected, suggesting that either UvrA or, more likely, UvrD1 plays a role in another process in addition to NER.

The enhanced susceptibility of the mutants was most pronounced for the nitrosative stress. This may be a consequence of deaminated bases resulting from NO exposure reacting with other cellular components to form adducts that require NER for their repair (34), while base damage caused by oxidative stress is also subject to repair by base excision repair (29). An *M. tuberculosis uvrB* mutant has been reported to exhibit a dramatic increase in susceptibility to nitrosative stress generated by acidified sodium nitrite (11, 12). The same authors found no significant increase in sensitivity to ROI (hydrogen peroxide, cumene hydroperoxide, or plumbagin) *in vitro* for their *uvrB* strain, as assessed using a disk diffusion assay. In contrast, *uvrB* mutants of *M. smegmatis* have been reported to exhibit enhanced susceptibility to ROI as well as RNI (22, 27), similar to the findings reported here for *M. tuberculosis*. However, the difference could be due to the different assays used in the studies.

There was no significant difference in the growth and survival of the *uvrA* mutant and that of the wild type within macrophages, indicating that NER is not required under these conditions. This could either be because significant DNA damage does not occur or, more likely, because other DNA repair mechanisms can compensate for the lack of NER. The *M. tuberculosis uvrB* mutant studied previously likewise exhibited only a slightly reduced ability to survive in BMDMs (12), although the infection conditions used in that study differed from those used here. In contrast, both the *uvrD1* and the *uvrA uvrD1* mutants exhibited reduced replication compared with the wild type following infection of macrophages.

The *uvrA uvrD1* mutant phenotype was significantly reversed by complementation of *uvrD1* alone. This would indicate that either both UvrA and UvrD must be inactivated to block the NER pathway, and/or there is an additional function for UvrD1 outside NER that is important for replication under intracellular conditions. This alternate function for UvrD1 during infection is supported by the less-pronounced phenotype that is observed for the *uvrD1* mutant to *in vitro* RNI stress compared to the *uvrA* mutant, in contrast to the relative ability of these strains to survive during infection.

Reactive nitrogen species produced by inducible nitric oxide synthase (iNOS) from IFN- $\gamma$  stimulation (17) play a strong role in controlling infection. Treatment of *M. tuberculosis*-infected mice with iNOS inhibitors given during acute or chronic infection caused mice to succumb to the disease (20, 36). Thus, there is a requirement for a functional NER and other DNA damage repair mechanisms during all stages of infection. Both types of mouse infection experiments conducted in this study demonstrated a striking attenuation throughout the course of infection when both *uvrA* and *uvrD1* were inactivated. The *uvrD1* single mutant showed attenuation at the later time points of infection, indicating a requirement for this protein in persistence, while the *uvrA* mutant was only modestly affected. In the study by Darwin and Nathan (12), the *uvrB* mutant exhibited a modest reduction in bacterial load during a mouse infection, analogous to that seen here for the *uvrA* mutant. The *uvrB* mutant was also shown to be at-

tenuated for growth in primate lungs (15), indicating the importance for NER during infection.

When *M. tuberculosis* from infected mouse lungs was analyzed by qRT-PCR for *uvrD1* expression, it was observed that there were increased transcript levels during infection compared to that found during *in vitro* growth. In particular, there was a dramatic increase of ca. 100-fold during late infection. As the requirement for *uvrD1* is increased in chronic infection, this would explain why the *uvrD1* mutant lacks the ability to persist at later time points.

Thus, it appears that UvrD1 is involved in processes separate from NER that are important for persistence in the absence of NER, while deletion of *uvrD1* alone is insufficient to fully inactivate NER.

The requirement for UvrD1 in pathogenesis in the absence of NER may reflect a role in replication restart or recombination. UvrD in *E. coli* or its homologue PcrA in *Bacillus subtilis* is important for replication restart (3, 19). It is thought that this action is at least partly mediated by the ability of these enzymes to restrict the actions of RecA at blocked replication forks (1, 31). Indeed, biochemical studies have shown that *M. tuberculosis* UvrD1 suppresses DNA strand exchange reactions catalyzed by RecA *in vitro* (46). UvrD homologues can also act as translocases, and in this way they are able to displace proteins bound to DNA (1). It is possible that translocase activity of *M. tuberculosis* UvrD1 could contribute to clearing RecA from the DNA at fork structures (9, 46). This behavior would be similar to that of the *E. coli* RecG helicase, which has been shown to be involved in the recovery of stalled replication forks (41). Although UvrD and RecG proteins are not homologues by sequence, they could have overlapping functions.

The studies described here suggest that targeting UvrD1 might be a potential strategy to combat persistence and that an inhibitor of UvrD1 would be particularly useful in combination with a compound such as one recently described (32) that targets an essential component of NER. Importantly, these results validate DNA repair processes in *M. tuberculosis* as potential new drug targets.

## ACKNOWLEDGMENTS

This work was supported by the European Community (CSI\_LTB LSHP-CT-2007-037235), the United Kingdom Medical Research Council (program number U1175 32056 to E.O.D.), and the University of Zurich (to E.C.B.).

We thank Bosco Chan for performing some preliminary phenotyping experiments and Belinda Dagg, James Keeble, and Biological Services at both NIMR and NIBSC for help with the mouse infection experiments.

## REFERENCES

1. Anand SP, Zheng H, Bianco PR, Leuba SH, Khan SA. 2007. DNA helicase activity of PcrA is not required for the displacement of RecA protein from DNA or inhibition of RecA-mediated strand exchange. *J. Bacteriol.* 189:4502–4509.
2. Barry CE, III, et al. 2009. The spectrum of latent tuberculosis: rethinking the biology and intervention strategies. *Nat. Rev. Microbiol.* 7:845–855.
3. Bidnenko V, Lestini R, Michel B. 2006. The Escherichia coli UvrD helicase is essential for Tus removal during recombination-dependent replication restart from Ter sites. *Mol. Microbiol.* 62:382–396.
4. Brosch R, et al. 1998. Use of a Mycobacterium tuberculosis H37Rv bacterial artificial chromosome library for genome mapping, sequencing, and comparative genomics. *Infect. Immun.* 66:2221–2229.
5. Burney S, Caulfield JL, Niles JC, Wishnok JS, Tannenbaum SR. 1999. The chemistry of DNA damage from nitric oxide and peroxynitrite. *Mutat. Res.* 424:37–49.
6. Cadenas E, Sies H. 1985. Oxidative stress: excited oxygen species and enzyme activity. *Adv. Enzyme Regul.* 23:217–237.

7. Chan ED, Chan J, Schluger NW. 2001. What is the role of nitric oxide in murine and human host defense against tuberculosis? Current knowledge. *Am. J. Respir. Cell Mol. Biol.* 25:606–612.
8. Cole ST, et al. 1998. Deciphering the biology of *Mycobacterium tuberculosis* from the complete genome sequence. *Nature* 393:537–544.
9. Curti E, Smerdon SJ, Davis EO. 2007. Characterization of the helicase activity and substrate specificity of *Mycobacterium tuberculosis* UvrD. *J. Bacteriol.* 189:1542–1555.
10. Czczot H, Tudek B, Lambert B, Laval J, Boiteux S. 1991. *Escherichia coli* Fpg protein and UvrABC endonuclease repair DNA damage induced by methylene blue plus visible light in vivo and in vitro. *J. Bacteriol.* 173:3419–3424.
11. Darwin KH, Ehrh S, Gutierrez-Ramos JC, Weich N, Nathan CF. 2003. The proteasome of *Mycobacterium tuberculosis* is required for resistance to nitric oxide. *Science* 302:1963–1966.
12. Darwin KH, Nathan CF. 2005. Role for nucleotide excision repair in virulence of *Mycobacterium tuberculosis*. *Infect. Immun.* 73:4581–4587.
13. Davis EO, et al. 2002. DNA damage induction of recA in *Mycobacterium tuberculosis* independently of RecA and LexA. *Molecular Microbiology* 46:791–800.
14. Davis EO, Forse LN. 2009. DNA repair: key to survival?, p 79–117. *In* Parish T, Brown A (ed), *Mycobacterium* genomics and molecular biology. Caister Academic Press, Wymondham, United Kingdom.
15. Dutta NK, et al. 2010. Genetic requirements for the survival of tubercle bacilli in primates. *J. Infect. Dis.* 201:1743–1752.
16. Dye C, Scheele S, Dolin P, Pathania V, Raviglione MC. 1999. Consensus statement. Global burden of tuberculosis: estimated incidence, prevalence, and mortality by country. WHO Global Surveillance and Monitoring Project. *JAMA* 282:677–686.
17. Ehrh S, Schnappinger D. 2009. Mycobacterial survival strategies in the phagosome: defence against host stresses. *Cell Microbiol.* 11:1170–1178.
18. Fivian-Hughes AS, Davis EO. 2010. Analyzing the regulatory role of the HgA antitoxin within *Mycobacterium tuberculosis*. *J. Bacteriol.* 192:4348–4356.
19. Florés MJ, Sanchez N, Michel B. 2005. A fork-clearing role for UvrD. *Mol. Microbiol.* 57:1664–1675.
20. Flynn JL, Scanga CA, Tanaka KE, Chan J. 1998. Effects of aminoguanidine on latent murine tuberculosis. *J. Immunol.* 160:1796–1803.
21. Frota CC, Papavinasandaram KG, Davis EO, Colston MJ. 2004. The AraC family transcriptional regulator Rv1931c plays a role in the virulence of *Mycobacterium tuberculosis*. *Infect. Immun.* 72:5483–5486.
22. Güthlein C, et al. 2009. Characterization of the mycobacterial NER system reveals novel functions of the uvrD1 helicase. *J. Bacteriol.* 191:555–562.
23. Iyer RR, Pluciennik A, Burdett V, Modrich PL. 2006. DNA mismatch repair: functions and mechanisms. *Chem. Rev.* 106:302–323.
24. Jung YJ, LaCourse R, Ryan L, North RJ. 2002. Virulent but not avirulent *Mycobacterium tuberculosis* can evade the growth inhibitory action of a T helper 1-dependent, nitric oxide synthase 2-independent defense in mice. *J. Exp. Med.* 196:991–998.
25. Kuemmerle NB, Masker WE. 1980. Effect of the uvrD mutation on excision repair. *J. Bacteriol.* 142:535–546.
26. Kumura K, Sekiguchi M, Steinum AL, Seeberg E. 1985. Stimulation of the UvrABC enzyme-catalyzed repair reactions by the UvrD protein (DNA helicase II). *Nucleic Acids Res.* 13:1483–1492.
27. Kurthkoti K, Kumar P, Jain R, Varshney U. 2008. Important role of the nucleotide excision repair pathway in *Mycobacterium smegmatis* in conferring protection against commonly encountered DNA-damaging agents. *Microbiology* 154:2776–2785.
28. Labes M, Puhler A, Simon R. 1990. A new family of RSF1010-derived expression and lac-fusion broad-host-range vectors for gram-negative bacteria. *Gene* 89:37–46.
29. Laval J. 1996. Role of DNA repair enzymes in the cellular resistance to oxidative stress. *Pathol. Biol.* 44:14–24.
30. Lestini R, Michel B. 2007. UvrD controls the access of recombination proteins to blocked replication forks. *EMBO J.* 26:3804–3814.
31. Mahdi AA, Buckman C, Harris L, Lloyd RG. 2006. Rep. and PriA helicase activities prevent RecA from provoking unnecessary recombination during replication fork repair. *Genes Dev.* 20:2135–2147.
32. Mazloum NA, et al. 2011. Identification of a chemical that inhibits the mycobacterial UvrABC complex in nucleotide excision repair. *Biochemistry* 50:1329–1335.
33. Mitić-Culafić D, et al. 2009. Protective effect of linalool, myrcene and eucalyptol against t-butyl hydroperoxide induced genotoxicity in bacteria and cultured human cells. *Food Chem. Toxicol.* 47:260–266.
34. Nakano T, et al. 2005. Repair activity of base and nucleotide excision repair enzymes for guanine lesions induced by nitrosative stress. *Nucleic Acids Res.* 33:2181–2191.
35. Nathan C, Shiloh MU. 2000. Reactive oxygen and nitrogen intermediates in the relationship between mammalian hosts and microbial pathogens. *Proc. Natl. Acad. Sci. U. S. A.* 97:8841–8848.
36. Nathan C. 2002. Inducible nitric oxide synthase in the tuberculous human lung. *Am. J. Respir. Crit. Care Med.* 166:130–131.
37. Nicholson S, et al. 1996. Inducible nitric oxide synthase in pulmonary alveolar macrophages from patients with tuberculosis. *J. Exp. Med.* 183:2293–2302.
38. Palyada K, et al. 2009. Characterization of the oxidative stress stimulon and PerR regulon of *Campylobacter jejuni*. *BMC Genomics* 10:481.
39. Reardon JT, Sancar A. 2005. Nucleotide excision repair. *Prog. Nucleic Acid Res. Mol. Biol.* 79:183–235.
40. Rossi F, et al. 2011. The biological and structural characterization of *Mycobacterium tuberculosis* UvrA provides novel insights into its mechanism of action. *Nucleic Acids Res.* 39:7316–7328.
41. Runyon GT, Bear DG, Lohman TM. 1990. *Escherichia coli* helicase II (UvrD) protein initiates DNA unwinding at nicks and blunt ends. *Proc. Natl. Acad. Sci. U. S. A.* 87:6383–6387.
42. Sambrook J, Fritsch E, Maniatis T. 1989. *Molecular cloning: a laboratory manual*, 2nd ed. Cold Spring Harbor Laboratory Press, Cold Spring Harbor, NY.
43. Sander P, Meier A, Bottger EC. 1995. rpsL+: a dominant selectable marker for gene replacement in mycobacteria. *Mol. Microbiol.* 16:991–1000.
44. Sander P, et al. 2001. *Mycobacterium bovis* BCG recA deletion mutant shows increased susceptibility to DNA-damaging agents but wild-type survival in a mouse infection model. *Infect. Immun.* 69:3562–3568.
45. Sidorkina O, Saparbaev M, Laval J. 1997. Effects of nitrous acid treatment on the survival and mutagenesis of *Escherichia coli* cells lacking base excision repair (hypoxanthine-DNA glycosylase-ALK A protein) and/or nucleotide excision repair. *Mutagenesis* 12:23–28.
46. Singh P, et al. 2010. *Mycobacterium tuberculosis* UvrD1 and UvrA proteins suppress DNA strand exchange promoted by cognate and noncognate RecA proteins. *Biochemistry* 49:4872–4883.
47. Sinha KM, Stephanou NC, Unciuleac MC, Glickman MS, Shuman S. 2008. Domain requirements for DNA unwinding by mycobacterial UvrD2, an essential DNA helicase. *Biochemistry* 47:9355–9364.
48. Springer B, Sander P, Sedlacek L, Ellrott K, Bottger EC. 2001. Instability and site-specific excision of integration-proficient mycobacteriophage L5 plasmids: development of stably maintained integrative vectors. *Int. J. Med. Microbiol.* 290:669–675.
49. Springer B, et al. 2004. Lack of mismatch correction facilitates genome evolution in mycobacteria. *Mol. Microbiol.* 53:1601–1609.
50. Stover CK, et al. 1991. New use of BCG for recombinant vaccines. *Nature* 351:456–460.
51. Truglio JJ, Croteau DL, Van Houten B, Kisker C. 2006. Prokaryotic nucleotide excision repair: the UvrABC system. *Chem. Rev.* 106:233–252.
52. Tufariello JM, Chan J, Flynn JL. 2003. Latent tuberculosis: mechanisms of host and bacillus that contribute to persistent infection. *Lancet Infect. Dis.* 3:578–590.
53. Washburn BK, Kushner SR. 1991. Construction and analysis of deletions in the structural gene (uvrD) for DNA helicase II of *Escherichia coli*. *J. Bacteriol.* 173:2569–2575.
54. World Health Organization. 2009. Global tuberculosis control: epidemiology, strategy, financing. WHO report 2009. World Health Organization, Geneva, Switzerland.